Decade-Bandwidth RF-Input Pseudo-Doherty Load-Modulated Balanced Amplifier Using Signal-Flow-Based Phase Alignment Design

Pingzhu Gong[®], Student Member, IEEE, Jiachen Guo, Student Member, IEEE, Niteesh Bharadwaj Vangipurapu[®], Student Member, IEEE, and Kenle Chen[®], Senior Member, IEEE

Abstract-This letter reports a first-ever decade-bandwidth pseudo-Doherty load-modulated balanced amplifier (PD-LMBA), designed for emerging 4G/5G communications and multiband operations. By revisiting the LMBA theory using the signalflow graph, a frequency-agnostic phase-alignment condition is found that is critical for ensuring intrinsically broadband load modulation (LM) behavior. This unique design methodology enables, for the first time, the independent optimization of broadband balanced amplifier (BA, as the peaking) and control amplifier (CA, as the carrier), thus fundamentally addressing the longstanding limits imposed on the design of wideband load-modulated power amplifiers (PAs). To prove the proposed concept, an ultra-wideband RF-input PD-LMBA is designed and developed using GaN technology covering the frequency range from 0.2 to 2 GHz. Experimental results demonstrate an efficiency of 51%-72% for peak output power and 44%-62% for 10-dB OBO, respectively.

Index Terms—Balanced amplifier (BA), Doherty, high efficiency, load modulation (LM), power amplifier (PA), signal-flow graph, wideband.

I. INTRODUCTION

TO MEET the ever-increasing demands for higher data rates and transmission capacity, sophisticated modulation schemes are used, resulting in signals with large-amplitude variations characterized by peak-to-average power ratio (PAPR). Consequently, power amplifiers (PAs), as the most power-hungry units in wireless communication systems, suffer from significant efficiency degradation. Moreover, given the proliferation of the wireless spectrum, PAs need to operate over a wide frequency range.

To address the inefficiency in transmission of signals with high PAPR, load modulation (LM) has emerged as an effective solution for PAs. Doherty power amplifier (DPA), as a representative of LM, has been extensively studied [1], [2] and widely adopted in base station applications. However, DPA is limited in providing a wide bandwidth due to the intrinsic constraints of the impedance inverter. On the other

Manuscript received 26 February 2024; revised 26 March 2024; accepted 9 April 2024. Date of publication 7 May 2024; date of current version 7 June 2024. This work was supported in part by the National Science Foundation under Award under Grant 1914875 and Grant 2218808. (Corresponding author: Kenle Chen.)

The authors are with the Department of Electrical and Computer Engineering, University of Central Florida, Orlando, FL 32816 USA (e-mail: pingzhu.gong@ucf.edu; kenle.chen@ucf.edu).

This article was presented at the IEEE MTT-S International Microwave Symposium (IMS 2024), Washington, DC, USA, June 16–21, 2024.

Color versions of one or more figures in this letter are available at https://doi.org/10.1109/LMWT.2024.3390585.

Digital Object Identifier 10.1109/LMWT.2024.3390585

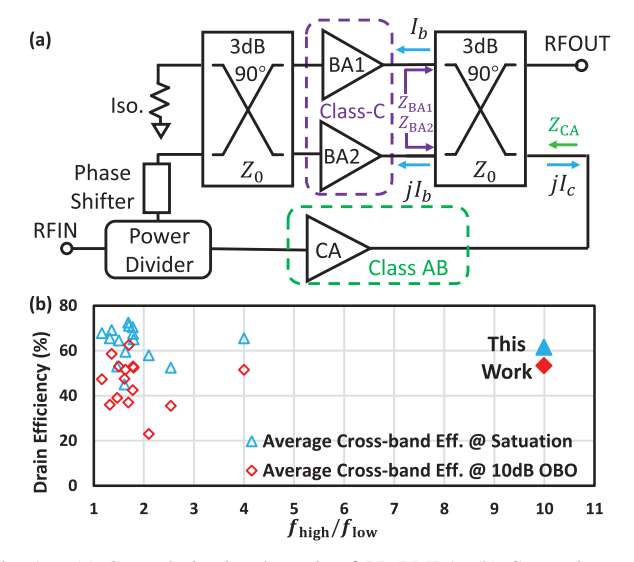


Fig. 1. (a) General circuit schematic of PD-LMBA. (b) Comparison with the state-of-the-art DPAs/LMBAs. (f_{high}/f_{low} refers to the ratio between the upper and lower boundaries of frequency range. Average cross-band efficiency is defined as the average of maximum and minimum efficiencies at a specific output power level).

hand, a recently introduced PA architecture, load-modulated balanced amplifier (LMBA) [3], has been demonstrated to provide both wide bandwidth and extended output power backoff (OBO) range. By injecting an additional signal into the isolation port of the output quadrature coupler of the balanced amplifier (BA) through another control amplifier (CA), the efficiency of BA is enhanced by LM. Furthermore, LMBA inherits the wideband nature of BA, offering a significant advantage over DPA. Developed from the original LMBA, a re-engineered LMBA mode is proposed, named as pseudo-Doherty load-modulated balanced amplifier (PD-LMBA) [4] or sequential load-modulated balanced amplifier (SLMBA) [5]. In PD-LMBA/SLMBA, the CA is set as the carrier device and the BA as peaking as shown in Fig. 1(a), enabling >10 dB of OBO range and ultra-wide bandwidth up to dual octaves (4:1) [6].

While LMBA is proven to be broadband in extensive experiments, no existing theory rigorously explains the consistency of LM across all the in-band frequencies. By constructing the full signal-flow graph of LMBA, this article demonstrates that LMBA can consistently exhibit broadband LM behavior when a specific CA-BA phase-alignment condition is met. The proposed theory and method are validated through the development of a PD-LMBA prototype. The bandwidth and

2771-957X © 2024 IEEE. Personal use is permitted, but republication/redistribution requires IEEE permission. See https://www.ieee.org/publications/rights/index.html for more information.

efficiency of the PD-LMBA prototype are then compared with DPAs and LMBAs reported in [1], [2], [4], [6], [7], [8], [9], [10], and [11], as illustrated in Fig. 1(b). Designed using the proposed theory, the bandwidth of the PD-LMBA prototype is broadened unprecedentedly to a decade, significantly outperforming the state-of-the-art.

II. PHASE-ALIGNMENT ANALYSIS BASED ON SIGNAL-FLOW GRAPH

The RF-input LMBA described in Fig. 1 consists of a BA and a control amplifier. In the LMBA theory, LM is described by [3], [4]

$$Z_{\text{BA1}} = Z_{\text{BA2}} = Z_0 \left(1 + \frac{\sqrt{2}I_c e^{j\theta}}{I_b} \right)$$
 (1)

where I_b and I_c are the magnitude of BA and CA currents, respectively, and θ is the phase of the control path. Note that the classical LMBA theory indicated by (1) does not involve any frequency dependence. In contrast, our proposed LMBA theory intrinsically accounts for frequency-dependent variations using the signal-flow graph. This analysis proves the consistent LM behavior of LMBA across all the in-band frequencies that solidly explains its wideband nature.

A. LMBA Revisited Using Signal-Flow Graph

The S-matrix of the wideband coupled-line coupler is given by

$$\begin{bmatrix} b_1 \\ b_2 \\ b_3 \\ b_4 \end{bmatrix} = \begin{bmatrix} 0 & jm & 0 & m \\ jm & 0 & m & 0 \\ 0 & m & 0 & jm \\ m & 0 & jm & 0 \end{bmatrix} \begin{bmatrix} a_1 \\ a_2 \\ a_3 \\ a_4 \end{bmatrix}$$
 (2)

where $m = (1/\sqrt{2})e^{j\theta(\omega)}$. While the phase of m is denoted by $\theta(\omega)$ representing its frequency dependence, the relationship of $S_{21} = jS_{41}$ consistently holds true. This implies that a 90° phase shift between the thru and coupled ports can be maintained across the entire frequency range of coupler.

The S-matrix of the transistor in a PA is expressed as

$$[S_{\text{Tr}}] = \begin{bmatrix} 0 & 0 \\ S_{21,\text{Tr}} & 1 \end{bmatrix}. \tag{3}$$

The transistor is modeled as an ideal voltage-controlled current source with infinite reverse isolation, and it is assumed to be matched at the input. Furthermore, the *S*-matrix of the input/output matching network of a PA is represented as

$$[S_{I/O}] = \begin{bmatrix} 0 & S_{12,I/O} \\ S_{21,I/O} & 0 \end{bmatrix}. \tag{4}$$

Both the input matching network (IMN) and output matching network (OMN) are assumed to be matched and reciprocal.

Based on the *S*-matrix of (2)–(4) and Fig. 1, the signal-flow graph of generic LMBA is depicted in Fig. 2, which can be viewed as the combination of two couplers and three sub-PAs with IMN and OMN included. Note that the device parasitics are considered as part of the OMN in (3). The *S*-matrix of the phase shifter can also be modeled by (4).

By applying Mason's rules [12] to the signal-flow graph of LMBA in Fig. 2, the output waves $(b_{\text{out,BA}}, b_{\text{out,CA}})$ induced by the BA and CA inputs $(a_{\text{BA}}, a_{\text{CA}})$ can be expressed as

$$b_{\text{out,BA}} = a_{\text{BA}} \cdot 2jm^2 S_{21,\text{PHS}} S_{21,\text{BI}} S_{21,\text{BTr}} S_{21,\text{BO}}$$

$$b_{\text{out,CA}} = a_{\text{CA}} \cdot 2jm^2 S_{21,\text{CI}} S_{21,\text{CTr}} S_{21,\text{CO}} S_{21,\text{BO}}^2$$
(5)

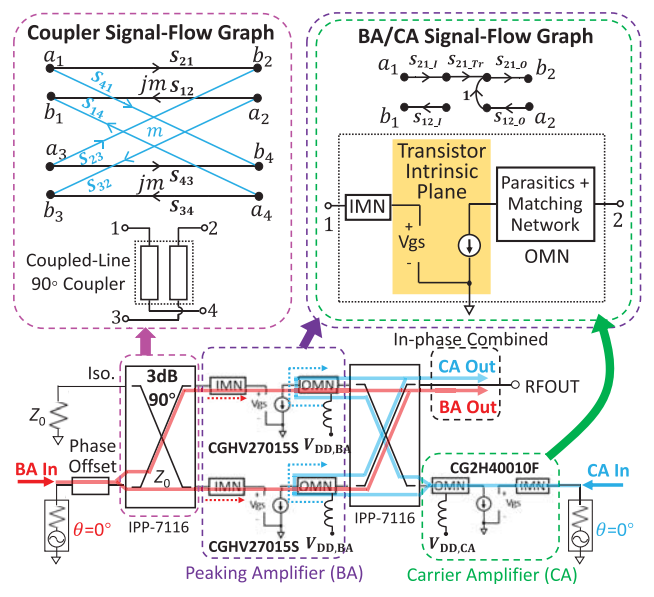


Fig. 2. Proposed signal-flow graph for the wideband PD-LMBA with circuit implementation using wideband coupled line couplers and GaN transistors.

where $S_{21,PHS}$ stands for the S_{21} of the phase shifter, and subscripts B and C refer to BA and CA, respectively (e.g., $S_{21,BI}$ denotes S_{21} of the BA IMN). The total output wave is a combination of BA and CA, i.e., $b_{out} = b_{out,BA} + b_{out,CA}$. In Fig. 2, the signal paths of BA (in red) and CA (in blue) are identified and visualized based on (5), similar to [7]. The common factor jm^2 implies that both the BA signal and CA signal pass through the coupler twice, resulting in the same phase delay, even though the phase of m is a function of frequency. The shared factor $S_{21,BO}$ indicates that the BA signal passes through the BA OMN once, while the CA signal traverses the BA OMN twice.

B. Frequency-Agnostic Phase Alignment for PD-LMBA

Given the ideal LM behavior of PD-LMBA, i.e., $\theta = 0^{\circ}$ in (1), BA and CA signals should be in-phase combined at the output. Eliminating the common factors in (5), the following condition needs to be satisfied:

$$\angle S_{21,PHS}S_{21,BI}S_{21,BTr} = \angle S_{21,CI}S_{21,CTr}S_{21,CO}S_{21,BO}.$$
 (6)

Note that (5) and (6) contain the frequency dependence of all the building blocks. If we assume the similar behavior of IMNs and transistors between BA and CA ($\angle S_{21,B1}S_{21,BTr} \approx \angle S_{21,C1}S_{21,CTr}$), the input phase shifter only needs to offset the combined phase of CA and BA OMNs ($\angle S_{21,C0}S_{21,B0} = \angle S_{21,PHS}$), so as to realize an inherently wideband PD-LMBA.

III. DESIGN OF DECADE-BANDWIDTH PD-LMBA

Based on the proposed theory, a 10-W GaN transistor (Wolfspeed CG2H40010F) is used for realizing the CA, while two 15-W GaN transistors (Wolfspeed CGHV27015S) are used for the BA in the PD-LMBA prototype. The realized circuit schematic is shown in Fig. 2. The target OBO is set to 10 dB to handle high-PAPR signals, and the target frequency range is from 0.2 to 2 GHz. Two identical 50- Ω wideband couplers (IPP-7116, Innovative Power Products) are used at the input and output of the BA, which provides the same phase delay for both BA and CA.

Device parasitics are extracted using the method reported in [13], with the intrinsic nodes of the transistor provided by the model. Subsequently, these device parasitics are used

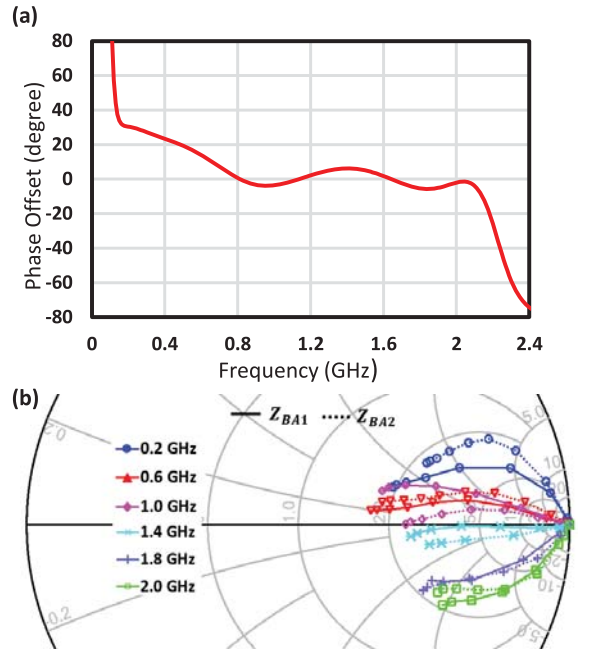


Fig. 3. (a) BA and CA signal path phase offset based on (6) at different frequencies. (b) BA intrinsic load impedance trajectories.

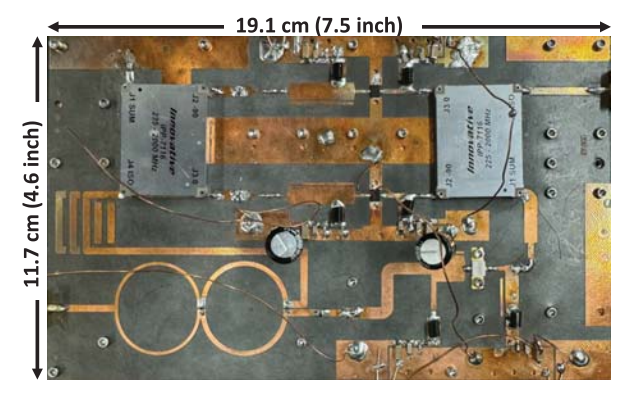


Fig. 4. Fabricated PD-LMBA prototype.

as part of OMN. Multisection-transformer-based matching network is used to realize BA and CA IMNs. Three RC-based networks (with $R = 200 \Omega$ and C = 10 pF) are incorporated into the IMNs to stabilize the PA. For CA OMN, a shunt open stub is added right after the transistor drain, along with two transmission lines in series, to collaborate with CA parasitics and establish the broadband multisection 40 Ω -50 Ω matching [1]. In addition, a short transmission line is introduced at the BA output to resonate with BA parasitics and provide 50 Ω –50 Ω matching. The IMNs and OMNs for both BAs and CAs are designed with the minimum number of shunt stubs to minimize phase dispersion, simplifying the phasealignment requirement described by (6). This allows us to add a transmission-line-based phase shifter at the BA input to properly align the phase of BA and CA paths. The phase offset between the BA and CA signal paths is plotted in Fig. 3(a), revealing that the phase difference in the proposed PD-LMBA is below 30° from 0.2 to 2 GHz. Fig. 3(b) displays the intrinsic load trajectories of BAs, indicating a desired LM behavior across all the in-band frequencies.

IV. IMPLEMENTATION AND EXPERIMENTAL RESULTS

The PA is implemented on a 31-mil thick Rogers Duroid-5880 PCB board with a dielectric constant of 2.2, as shown in Fig. 4. The CA is biased in Class-AB with $V_{\rm DD,CA}$

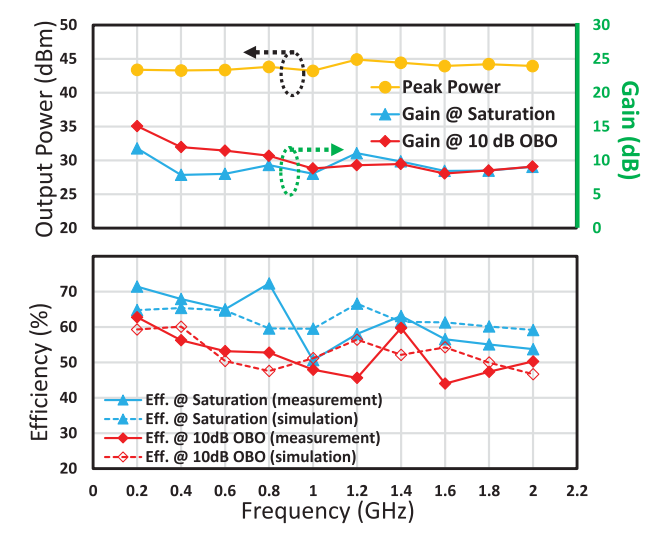


Fig. 5. Measured peak output power, gain, and efficiency at various OBO levels from 0.2 to 2 GHz.

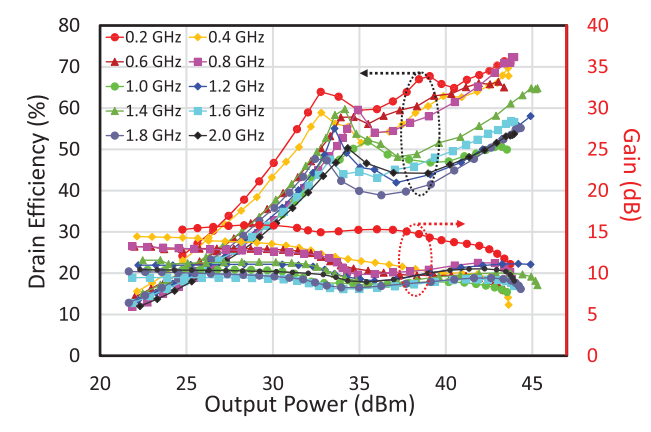


Fig. 6. Power-swept measurement of efficiency and gain from 0.2 to 2 GHz.

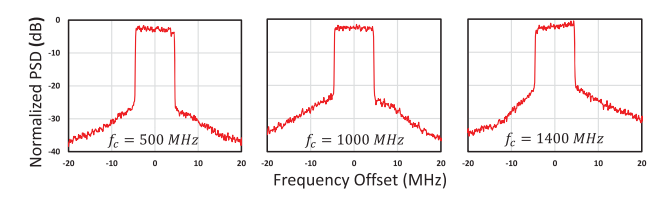


Fig. 7. Output spectrum from modulated measurement using a 10-MHz 9.5-dB-PAPR LTE signal centered at 500, 1000, and 1400 MHz.

around 12 V. The BA is biased in Class-C with 50-V $V_{\rm DD,BA}$. Bias voltages are adjusted to improve the PA performance at different frequencies. The prototype is tested using both continuous-wave (CW) and modulated signals.

A. CW Measurement

The PD-LMBA prototype is evaluated using a single-tone signal across the frequency range of 0.2–2 GHz at various power levels. The frequency response is shown in Fig. 5. A peak output power ranging from 43 to 45 dBm is observed across the entire bandwidth, along with a gain of 9–15 dB at different OBO levels. The corresponding measured peak efficiency falls within the range of 51%–72%, and the efficiencies at 10 dB OBOs are in the range of 44%–62%. The power-dependent gain and efficiency profiles at various frequencies are shown in Fig. 6, which indicates a strong efficiency enhancement across different power levels. $V_{\rm GS,BA1}$ and $V_{\rm GS,BA2}$ are set unequal at some frequencies to further

improve the back-off efficiency between the peak power and 10-OBO [14], e.g., 0.2 GHz in Fig. 6.

B. Modulated Measurements

A 10-MHz-bandwidth LTE signal with a PAPR of 9.5 dB is used to perform modulated measurement. The modulated signals are generated and analyzed using Keysight PXIe vector transceiver (VXT M9421). The average power of the modulated signals is 34 dBm, and the output spectrum is shown in Fig. 7 at 500, 1000, and 1400 MHz, with average efficiency of 52%, 48%, and 49%, respectively. The measured adjacent channel leakage ratios (ACLRs) at these frequencies are higher than 22 dB, and no digital predistortion (DPD) is performed.

V. CONCLUSION

This letter presents a comprehensive analysis of LMBA from a signal-flow perspective. By constructing the full signalflow graph of LMBA, it is, for the first time, demonstrated that the LM behavior of LMBA can be sustained across all the in-band frequencies when a specific BA-CA phase alignment condition is met. This finding not only provides a rigorous explanation of the wideband nature of LMBA but also introduces a novel design methodology for realizing ultra-wideband LMBAs. Moreover, the signal-flow approach offers the opportunity to analyze the behavior of other loadmodulated PA topologies from a new perspective. To prove the proposed concept, an ultra-wideband RF-input PD-LMBA is designed and developed using GaN technology covering the frequency range from 0.2 to 2 GHz. The experimental results demonstrate an efficiency of 51%-72% for peak output power and 44%–62% for 10-dB OBO, respectively. By leveraging the BA-CA phase alignment condition identified in this study, the bandwidth of the PD-LMBA prototype has been extended to an unprecedented decade-wide range, significantly outperforming the state-of-the-art.

ACKNOWLEDGMENT

The authors would like to thank Prof. Patrick Roblin of The Ohio State University for his insightful signal-flow graph of the BA from his lecture slides. The authors also want to thank Ryan Baker of Wolfspeed (now MACOM) for providing transistor samples.

REFERENCES

- [1] J. J. M. Rubio, V. Camarchia, M. Pirola, and R. Quaglia, "Design of an 87% fractional bandwidth Doherty power amplifier supported by a simplified bandwidth estimation method," *IEEE Trans. Microw. Theory Techn.*, vol. 66, no. 3, pp. 1319–1327, Mar. 2018.
- [2] Y. Xu, J. Pang, X. Wang, and A. Zhu, "Enhancing bandwidth and back-off range of Doherty power amplifier with modified load modulation network," *IEEE Trans. Microw. Theory Techn.*, vol. 69, no. 4, pp. 2291–2303, Apr. 2021.
- [3] D. J. Shepphard, J. Powell, and S. C. Cripps, "An efficient broadband reconfigurable power amplifier using active load modulation," *IEEE Microw. Wireless Compon. Lett.*, vol. 26, no. 6, pp. 443–445, Jun. 2016.
- [4] Y. Cao and K. Chen, "Pseudo-Doherty load-modulated balanced amplifier with wide bandwidth and extended power back-off range," *IEEE Trans. Microw. Theory Techn.*, vol. 68, no. 7, pp. 3172–3183, Jul. 2020.
- [5] J. Pang et al., "Analysis and design of highly efficient wideband RF-input sequential load modulated balanced power amplifier," *IEEE Trans. Microw. Theory Techn.*, vol. 68, no. 5, pp. 1741–1753, May 2020.
- [6] Y. Cao, H. Lyu, and K. Chen, "Asymmetrical load modulated balanced amplifier with continuum of modulation ratio and dual-octave bandwidth," *IEEE Trans. Microw. Theory Techn.*, vol. 69, no. 1, pp. 682–696, Jan. 2021.
- [7] J. Guo, Y. Cao, and K. Chen, "1-D reconfigurable pseudo-Doherty load modulated balanced amplifier with intrinsic VSWR resilience across wide bandwidth," *IEEE Trans. Microw. Theory Techn.*, vol. 71, no. 6, pp. 2465–2478, Jun. 2023.
- [8] C. Chu, J. Pang, R. Darraji, S. K. Dhar, T. Sharma, and A. Zhu, "Broad-band sequential load modulated balanced amplifier with extended design space using second harmonic manipulation," *IEEE Trans. Microw. Theory Techn.*, vol. 71, no. 5, pp. 1990–2003, May 2023.
- [9] C. Belchior, L. C. Nunes, P. M. Cabral, and J. C. Pedro, "Sequential LMBA design technique for improved bandwidth considering the balanced amplifiers off-state impedance," *IEEE Trans. Microw. Theory Techn.*, vol. 71, no. 8, pp. 3629–3643, Aug. 2023.
- [10] C. Liang, P. Roblin, Y. Hahn, J. I. Martinez-Lopez, H.-C. Chang, and V. Chen, "Single-input broadband hybrid Doherty power amplifiers design relying on a phase sliding-mode of the load modulation scheme," *IEEE Trans. Microw. Theory Techn.*, vol. 71, no. 4, pp. 1550–1562, Apr. 2023.
- [11] J. Xia, W. Chen, F. Meng, C. Yu, and X. Zhu, "Improved three-stage Doherty amplifier design with impedance compensation in load combiner for broadband applications," *IEEE Trans. Microw. Theory Techn.*, vol. 67, no. 2, pp. 778–786, Feb. 2019.
- [12] D. M. Pozar, Microwave Engineering, 3rd ed. Hoboken, NJ, USA: Wiley, 2005. [Online]. Available: https://cds.cern.ch/record/882338
- [13] P. Gong, "Design of a broadband Doherty power amplifier with a graphical user interface tool," M.S. thesis, Dept. Elect. Comput. Eng., Ohio State Univ., Columbus, OH, USA, 2022. [Online]. Available: http://rave.ohiolink.edu/etdc/view?acc_num=osu1658158564568844
- [14] Y. Cao, H. Lyu, and K. Chen, "Continuous-mode hybrid asymmetrical load-modulated balanced amplifier with three-way modulation and multi-band reconfigurability," *IEEE Trans. Circuits Syst. I, Reg. Papers*, vol. 69, no. 3, pp. 1077–1090, Mar. 2022.